

Applying experimental constraints to a one-dimensional model for BiS₂ superconductivity

M. A. Griffith,^{1,*} K. Foyevtsova,^{2,3} M. A. Continentino,¹ and G. B. Martins^{4,†}

¹*Centro Brasileiro de Pesquisas Físicas, Rua Dr. Xavier Sigaud 150, Urca, 22290-180 Rio de Janeiro, RJ, Brazil*

²*Department of Physics & Astronomy, University of British Columbia, Vancouver, British Columbia V6T 1Z1, Canada*

³*Quantum Matter Institute, University of British Columbia, Vancouver, British Columbia V6T 1Z4, Canada*

⁴*Department of Physics, Oakland University, Rochester, MI 48309, USA*

Recent ARPES measurements [Phys. Rev. B **92**, 041113 (2015)] have confirmed the one-dimensional character of the electronic structure of CeO_{0.5}F_{0.5}BiS₂, a representative of BiS₂-based superconductors. In addition, several members of this family present sizable increase in the superconducting transition temperature T_c under application of hydrostatic pressure. Motivated by these two results, we propose a one-dimensional three-orbital model, whose kinetic energy part, obtained through *ab initio* calculations, is supplemented by pair-scattering terms, which are treated at the mean-field level. We solve the gap equations self-consistently and then systematically probe which combination of pair-scattering terms gives results consistent with experiment, namely, a superconducting dome with a maximum T_c at the right chemical potential and a sizable increase in T_c when the magnitude of the hoppings is increased. For these constraints to be satisfied multi-gap superconductivity is required, in agreement with experiments, and one of the hoppings has a dominant influence over the increase of T_c with pressure.

PACS numbers: 74.20.Mn, 74.20.Rp, 74.70.-b

Introduction. After the discovery of the cuprates in 1986¹, the search for new layered superconducting materials has attracted much attention, with important discoveries occurring in the last 15 years. For example, it was discovered in 2001 that MgB₂ has $T_c = 39$ K² and in 2008 superconductivity (SC) in the iron pnictides was reported³. Both MgB₂ and the iron pnictides have highlighted the importance of multiband SC⁴, to the point that the recent literature on cuprates devoted to multiband models has substantially increased⁵. An unrelated development has been the explosion of research in topological superconductors⁶, due to proposals to ‘engineer’ Majorana fermion quasiparticles through midgap excitations of a chiral p-wave superconductor. This has led to renewed interest in the Ruthenate compound Sr₂RuO₄, discovered in 1994⁷, which is one of the few candidates to realizing p-wave-type SC^{8,9}, another candidate being the organic superconductor (TMTSF)₂PF₆. It should also be emphasized that, as was the case for intermetallics with A15 structure (like Nb₃Sn or V₃Si)¹⁰, the Ruthenates display ‘hidden’ quasi-one-dimensional (quasi-1d) SC¹¹ (while organic superconductors are explicitly 1d). Finally, we also mention SC in doped semiconductors, studied since before the 60s¹², with the interest greatly increasing after the discovery of SC in Boron-doped Diamond with $T_c = 4$ K¹³.

It is then interesting that one of the latest families of layered superconductors to be discovered, those containing BiS₂ planes,¹⁴ presents many of the characteristics mentioned above: a layered structure, similar to cuprates and pnictides¹⁵; a double superconducting gap as in MgB₂¹⁶; its minimal model contains two bands¹⁷, and Fermi surface nesting effects seem to be important¹⁸ (as in the iron pnictides); because it contains a heavy element (Bismuth), spin-orbit effects are enhanced and some proposals linking BiS₂ to spin-triplet pairing and a weak topological superconducting state have been made¹⁹; based on first-principles electronic structure calculations, it has been pointed out the ‘subtle’ 1d character of its band structure¹⁷, which has been recently confirmed exper-

imentally through polarization-dependent Angular Resolved Photoemission Spectroscopy (ARPES) measurements²⁰; finally, a few members of the BiS₂ family have semiconducting parent compounds that become metallic/superconducting with electron doping or application of moderate hydrostatic pressure, which also can lead to sizable increase in T_c ²¹.

In this work, to advance the understanding of SC in BiS₂, where there is no consensus yet if it is of the conventional or unconventional type²², we concentrate in these last two aspects: one-dimensionality of the electronic structure and the pronounced effects pressure has over the superconducting phase. To model that, the authors take the following approach: i) adopt a 1d three-orbital model for BiS₂, adding the Cooper-pairing by hand, ii) solve the gap equations at the mean-field level, iii) study the dependence of the superconducting gap with the variation of the hopping terms, whose magnitude one expects to increase under applied pressure iv) decide on the acceptance or not of specific pair-scattering terms based on semi-quantitative agreement with experiments. Regarding this last point, we look specifically in what range of electron-filling a superconducting dome is obtained (see Fig. 3) and how SC varies with hopping parameters. To make the connection with BiS₂ more explicit, and thus obtain semi-quantitative agreement with experiments, all the parameter values of the single-particle Hamiltonian were obtained through first-principles Density Functional Theory (DFT) calculations for a two-dimensional (2d) five-band model (see Table I).

We can summarize our results as follows: Taking into account a three-orbital model, where Sulfur contributes with orbitals *s* and *p*, and Bismuth with a *p* orbital (see Fig. 1), we considered all possible pair-scattering terms (intra and interband, restricted to pairs formed by same-band electrons), individually and in conjunction, and solved the resulting gap equations at the mean-field level. We obtain that i) no single-band pair-scattering process, acting isolatedly, can describe the experiments (as specifically defined above), unless an un-

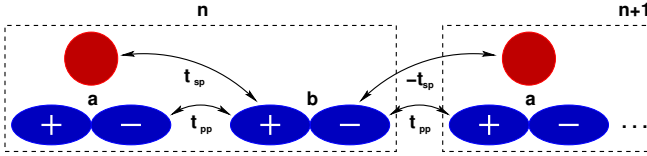


FIG. 1: 1d model for BiS_2 . t_{pp} and t_{sp} are the hopping terms considered in our model. The dashed box indicates the unit cell with atoms a (Sulfur, with orbitals s and p) and b (Bismuth, with just one p orbital). Notice the alternating signs of the t_{sp} hoppings²³.

TABLE I: Partial list of tight-binding parameters (in eV) for the 2d five-orbital model. The same parameters are used for the 1d three-orbital model depicted in Fig. 1. The chemical potential corresponds to 1/8-filling of the p_b orbital in the 1d model.

$\epsilon_{s,n}$	$\epsilon_{p_a,n}$	$\epsilon_{p_b,n}$	t_{sp}	t_{pp}	μ
-11.2840	-1.2691	0.1635	-0.9952	-0.8155	0.5007

realistic coupling is assumed ($g > 0.1$ eV); this seems to indicate that multi-gap SC is a natural consequence of our model ii) two different types of multi-gap SC (see detailed description below) are in semi-quantitative agreement with experiments iii) the gap dependence with hopping (see Fig. 4) indicates a qualitative difference between the two hoppings considered in our model. These important results establish an appropriate effective 1d model to simulate the properties of BiS_2 . We expect that our work will motivate other groups to investigate other similar purely 1d effective models.

Model. We consider a linear chain with a unit cell consisting of two sites denoted a and b , see Fig. 1. The a sites (Sulfur) have orbitals s and p , while b sites (Bismuth) have just one p orbital. In second quantization notation, the annihilation operator for an s orbital in unit cell n is denoted as c_n , and those for Sulfur and Bismuth p orbitals are denoted $p_{a,n}$ and $p_{b,n}$, respectively. The non-interacting part of the Hamiltonian can then be written as

$$\begin{aligned} \mathcal{H} = & \sum_n \{ (\epsilon_{s,n} + \mu) n_{s,n} + \sum_{i=a,b} (\epsilon_{p_i,n} + \mu) n_{p_i,n} \\ & + t_{pp} [p_{a,n}^\dagger p_{b,n} + p_{b,n}^\dagger p_{a,n+1} + \text{h.c.}] \\ & + t_{sp} [c_n^\dagger p_{b,n} - p_{b,n}^\dagger c_{n+1} + \text{h.c.}] \} \end{aligned} \quad (1)$$

where $\epsilon_{s,n}$ and $\epsilon_{p_i,n}$ describe the energy levels of orbitals s and p (for site $i = a, b$) at unit cell n , respectively; $n_{s,n} = c_n^\dagger c_n$ and $n_{p_i,n} = p_{i,n}^\dagger p_{i,n}$ are the number operators, and μ is the chemical potential. The hopping parameters are indicated in Fig. 1 and the values used in this work (along with orbital energies and chemical potential) are listed in Table I in eV units. Note that these parameter values were obtained through a full DFT calculation. The hoppings kept for the 1d model here studied were all the nearest neighbor hoppings in excess of 0.5 eV.

An early 2d minimal model for BiS_2 contains two orbitals: Bismuth p_x and p_y orbitals¹⁷. Therefore, before deriving the self-consistent gap equations, the inclusion of the Sulfur p and

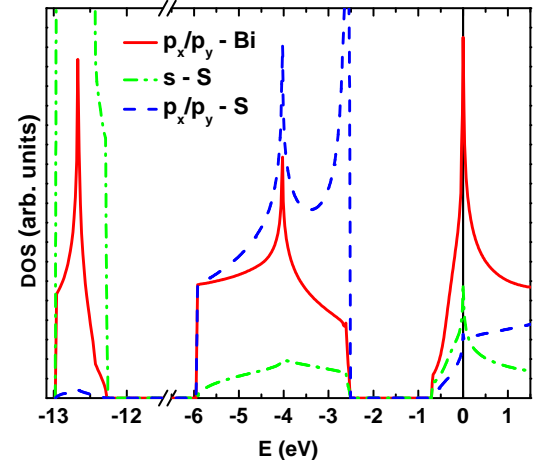


FIG. 2: Density of states obtained through DFT for the five-orbital model of the LaOBiS_2 compound. Note the importance of the Sulfur s -orbitals [dot-dashed (green) line] at the Fermi energy ($E_F = 0$), justifying its inclusion in the model described in Fig. 1. In addition, the sequence of van Hove singularities at the bottom of the conduction band and at the top of the valence band indicates the quasi-1d character of the electronic structure.

s orbitals should be justified, mainly the latter one, which lies deep below the Fermi energy (see DFT parameter values in Table I). Figure 2 shows the density of states (DOS) obtained for a 2d model of BiS_2 involving five orbitals: two Bismuth p orbitals (p_x and p_y), two Sulfur p orbitals (p_x and p_y), and one Sulfur s orbital. From the examination of the DOS one can conclude that, at the Fermi energy $E_F = 0$ (which, in this plot, is between 1/8- and 1/4-filling, for the 2d model), the participation of the Sulfur s orbital [dot-dashed (green) curve], is quite relevant, even more than that of the Sulfur p orbitals [dashed (blue) curve]. In addition, it is easy to recognize the characteristic 1d DOS profile for the Sulfur p orbital at the top of the valence band and for the Bismuth p and Sulfur s orbitals at the bottom of the conduction band. This, coupled to the above mentioned polarized ARPES results indicating the one-dimensionality of the electronic structure of BiS_2 , justifies our model. We now proceed to the derivation of the self-consistent gap equations.

Self-consistent gap equations at zero temperature. After taking a Fourier transform of the non-interacting part, and introducing pair-scattering terms between the electrons, the total Hamiltonian can be written as

$$\begin{aligned} \mathcal{H}(k) = & \sum_k \{ (\epsilon_{as} + \mu) c_k^\dagger c_k + \sum_{i=a,b} (\epsilon_{p_i} + \mu) p_{ik}^\dagger p_{ik} \\ & + 2t_{pp} \cos(k) [p_{ak}^\dagger p_{bk} + \text{h.c.}] \\ & + 2it_{sp} \sin(k) [c_k^\dagger p_{bk} - \text{h.c.}] \\ & - \sum_{i,j,k,k'} g_{ij} [\gamma_{i,k+}^\dagger \gamma_{i,\bar{k}-}^\dagger \gamma_{j,k'+} \gamma_{j,\bar{k}'-} + \text{h.c.}] \} \end{aligned} \quad (2)$$

where, in the last line, $\gamma_{i,j,k\sigma}$ ($\sigma = \pm$ and \bar{k} indicates $-k$)

stands for either one of $c_{k\sigma}$, $p_{a,k\sigma}$, or $p_{b,k\sigma}$. Note that it is implicit in the form of the expression for the pair-scattering term that we are only considering Cooper pairs composed of electrons from the same band, as pairing of different-band electrons tends to promote pair-density-waive (inhomogeneous) superconducting ground states²⁴. Already anticipating results that will be discussed below (see Fig. 3), we describe how to obtain the gap equations when an specific set of pair-scattering processes are taken in account. Considering terms involving *intraband* scattering in the s and p_b bands and *interband* scattering between the s and p_b bands, the last line of eq. (2) (which we denote as Δ^{SC}) can be written as

$$\begin{aligned} \Delta^{SC} = & - \sum_k \{ g_{ss} [c_{k+}^\dagger c_{\bar{k}-}^\dagger c_{\bar{k}-} c_{k+}] \\ & + g_{p_b p_b} [p_{b,k+}^\dagger p_{b,\bar{k}-}^\dagger p_{b,\bar{k}-} p_{b,k+}] \\ & + g_{sp_b} [c_{k+}^\dagger c_{\bar{k}-}^\dagger p_{b,\bar{k}-} p_{b,k+}] \\ & + p_{b,k+}^\dagger p_{b,\bar{k}-}^\dagger c_{\bar{k}-} c_{k+}] \}. \end{aligned} \quad (3)$$

Note that, for simplicity, we consider the pairing couplings g_{ij} as being k -independent, *i.e.*, we assume s-wave pairing functions. Applying a mean-field decoupling eq. (3) becomes

$$\begin{aligned} \Delta^{SC} = & - \sum_k \{ \Delta_{ss} (c_{\bar{k}-} c_{k+} + c_{k+}^\dagger c_{\bar{k}-}^\dagger) \\ & + \Delta_{p_b p_b} (p_{p,\bar{k}-} p_{b,k+} + p_{b,k+}^\dagger p_{b,\bar{k}-}^\dagger) \\ & + [\Delta'_{ss} (p_{b,\bar{k}-} p_{b,k+} + p_{b,k+}^\dagger p_{b,\bar{k}-}^\dagger) \\ & + \Delta'_{p_b p_b} (c_{k+}^\dagger c_{\bar{k}-}^\dagger + c_{\bar{k}-} c_{k+})] \}, \end{aligned} \quad (4)$$

which can be rewritten as

$$\begin{aligned} \Delta^{SC} = & - \sum_k \Delta_1 (c_{\bar{k}-} c_{k+} + c_{k+}^\dagger c_{\bar{k}-}^\dagger) \\ & + \Delta_2 (p_{p,\bar{k}-} p_{b,k+} + p_{b,k+}^\dagger p_{b,\bar{k}-}^\dagger), \end{aligned} \quad (5)$$

with the following definitions

$$\begin{aligned} \Delta_1 &= \Delta_{ss} + \Delta'_{p_b p_b} \\ &= g_{ss} \sum_k \langle c_{\bar{k}-} c_{k+} \rangle + g_{sp_b} \sum_k \langle p_{b,\bar{k}-} p_{b,k+} \rangle \end{aligned}$$

and

$$\begin{aligned} \Delta_2 &= \Delta'_{ss} + \Delta_{p_b p_b} \\ &= g_{sp_b} \sum_k \langle c_{\bar{k}-} c_{k+} \rangle + g_{p_b p_b} \sum_k \langle p_{b,\bar{k}-} p_{b,k+} \rangle, \end{aligned}$$

where $\langle \rangle$ indicates an average over the ground state. For simplicity, if we consider the following relations, $g_{ss} = g_{p_b p_b} = g_{sp_b} = g$ and $\Delta_{ss} = \Delta'_{ss} = \Delta_{p_b p_b} = \Delta'_{p_b p_b} = \Delta$, we obtain the gap equation as

$$2\Delta = g \sum_k (\langle c_{\bar{k}-} c_{k+} \rangle + \langle p_{b,\bar{k}-} p_{b,k+} \rangle). \quad (6)$$

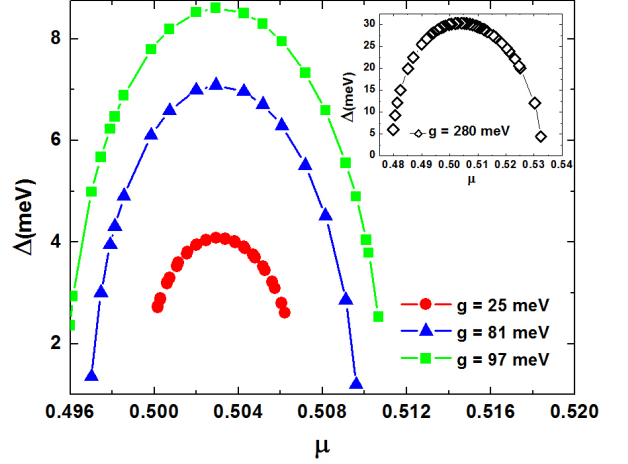


FIG. 3: Pairing interaction Δ as a function of the chemical potential μ for different values of the coupling constant g . These results were obtained for the tight-binding parameter values listed in Table I. The value of μ at the center of the dome corresponds to an electron filling close to the one in BiS_2 compounds where SC has been observed (1/8-filling). The inset shows results for a larger value of g , which stabilizes the superconducting phase in a much broader interval of μ .

We want to derive a self-consistent equation for Δ and then analyze the effect of variations in the hopping parameters over it. In order to determine the correlations $\langle c_{\bar{k}-} c_{k+} \rangle$ and $\langle p_{b,\bar{k}-} p_{b,k+} \rangle$ in the gap equation, we need to calculate the anomalous Green's functions $\langle \langle c_{k+}; c_{\bar{k}-} \rangle \rangle$ and $\langle \langle p_{b,k+}; p_{b,\bar{k}-} \rangle \rangle$. These calculations are long and tedious, and thus are presented in the supplemental material²⁵. After writing the equation of motion for the propagators $\langle \langle p_{b,k+}; p_{b,\bar{k}-} \rangle \rangle$ and $\langle \langle c_{k+}; c_{\bar{k}-} \rangle \rangle$, and through lengthy algebraic manipulations, we arrive at expressions for Δ_1 and Δ_2

$$\begin{aligned} \Delta_{1;2} = & - g_{ss;sp_b} k_f \pi \int_{-1}^1 d\tilde{k} \sum_{j=1}^3 \frac{|D_{ss}(-\omega_{\tilde{k},j})|}{\omega_{\tilde{k},j} r_j} \\ & - g_{sp_b;p_b p_b} k_f \pi \int_{-1}^1 d\tilde{k} \sum_{j=1}^3 \frac{|D_{p_b p_b}(-\omega_{\tilde{k},j})|}{\omega_{\tilde{k},j} r_j} \end{aligned} \quad (7)$$

which, after the simplifying step mentioned above, results in $\Delta_1 = \Delta_2 = \Delta$ (the terms under the two integrals are fully developed in the supplemental material²⁵).

Results. As mentioned in the Introduction, our strategy was to solve the gap equations at the mean-field level (hopping amplitudes fixed at the values obtained by DFT), and look for solutions at least qualitatively compatible with experiments, *i.e.*, for chemical potential values around 1/8-filling and for coupling strengths g that are not unrealistically large. Taking in account the pair-scattering terms in eq. (4) and following the derivations up to eq. (7), we obtain the gap function Δ , which has a dependence with μ as shown in Fig. 3, for three different values of coupling g . It is interesting to note that the value of μ around which the three domes are centered corresponds to

an electron filling close to that where SC has been found for most members of the BiS₂ family, i.e., 1/8-filling²⁶. This is an important result, as μ was *not* fixed from the start. It is taken as a free parameter, whose value, obtained self-consistently, was used to determine which gap equations (for specific pair-scattering terms) produced acceptable results. Indeed, if the value of μ for which SC was found is too far removed from 1/8-filling, that gap equation (and the pair-scattering term generating it) is rejected.

If one takes the maximum value obtained for Δ in Fig. 3 for $g = 25$ meV [(red) circles], $\Delta \approx 4$ meV, and uses the BCS relation $2\Delta/k_B T_c = 3.52$, one obtains $T_c \approx 26$ K. A maximum $T_c \approx 11$ K has been found for LaO_{1-x}F_xBiS₂ at 1/8-filling ($x = 0.5$)²⁷, indicating that our results, for a realistic value of g , produce a T_c qualitatively similar to experiments. A comment should be made on the horizontal width of the dome for the (red) solid circles curve in Fig. 3. At the base of the dome, the electron filling varies roughly from 0.25 to 0.26 electrons per p_b -orbital (Bismuth). Although there is still some controversy about the actual filling around which SC occurs²⁶, a few of the published T_c vs. doping results indicate a broader dome. We believe that the narrower dome we obtain is an artifact of the 1d model. Indeed, the DOS close to 1/8-filling for our 1d model (not shown) has a very pronounced van Hove singularity, therefore a very strong variation of DOS with the chemical potential. This strong dependence, for smaller values of g (as the ones plotted in the main panel in Fig. 3), seems to result in a superconducting phase that is very sensitive to the chemical potential, leading to a narrow dome. In the inset to Fig. 3, we show results for a larger $g = 280$ meV value. In it, we see a much broader variation in electron filling, from 0.2 to 0.31 [(black) open diamonds curve]. The actual system is quasi-1d, implying that once a three-dimensional superconducting state stabilizes, it will be less sensitive to variations in the chemical potential. To have the same effect in a purely 1d model we have to increase the pairing coupling, as shown in the inset to Fig. 3.

It is reasonable to expect that applying hydrostatic pressure in a crystal lattice will enhance the overlap between the orbitals and therefore increase the magnitude of the hopping terms. Taking the reasonable assumption that this increase is similar to the change in lattice parameter, which for an applied pressure of 2 GPa will amount to a change of $\approx 1\%$ ²⁸, we solve the gap equations for increasing values (in magnitude) of t_{sp} and plot the results in Fig. 4 for some μ values in the dome region in Fig. 3 (for $g = 81$ meV). For a variation of $|t_{sp}| \approx 0.5\%$ the value of Δ roughly doubles, which is in semi-quantitative agreement with experimental results for T_c obtained for LaO_{0.5}F_{0.5}BiS₂ and CeO_{0.5}F_{0.5}BiS₂²⁹. A similar calculation for the variation in t_{pp} (not shown) shows no changes in Δ , up to the same percent variation as for t_{sp} . This seems to be consistent with previous results²³ showing that antisymmetric hybridization is very effective in increasing the SC gap amplitude. To test this hypothesis, extensive calculations are underway where the condition $g_{ss} = g_{pbpb} = g_{spb} = g$ is relaxed³⁰.

There is another choice of pair-scattering terms in eq. (4) which produces results (not shown) very similar to the ones

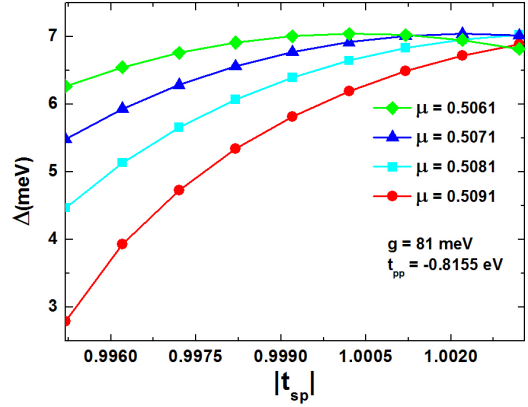


FIG. 4: Results showing the dependence of Δ with t_{sp} for a few values of the chemical potential μ in the dome region in Fig. 3 for $g = 81$ meV and $t_{p_a p_b} = -0.8155$ eV. The overall variation in the magnitude of t_{sp} is $\approx 0.4\%$, which is a typical lattice parameter variation under typical hydrostatic pressure experiments.

just described. One just needs to replace s by p_a in eq. (4). As already mentioned, these two were the only situations where the results obtained were compatible with the criteria described above for acceptance of the gap equation results. For all the other possibilities, either the coupling parameter g was unrealistically large or the electron-filling was too far removed from 1/8-filling.

Conclusions. Motivated by recent experiments in superconducting members of the BiS₂ family of compounds showing its ‘hidden’ 1d electronic structure and the strong effect that pressure has over its superconducting state, we propose an effective 1d model where the kinetic energy part of the Hamiltonian is obtained through DFT calculations for the 2d model for BiS₂. Supported by the DOS results shown in Fig. 2, we add the Sulfur p- and s-orbital to the p-orbital of Bismuth. Despite being several eV below the other two orbitals, the s-orbital undergoes strong hybridization with the Bismuth p-orbital and has a sizable contribution to the DOS at the Fermi energy, justifying its inclusion in the model (see Figs. 1 and 2). Pair scattering terms are then added and treated at the mean-field level. We solve the gap equations and systematically probe what combination of pair-scattering terms produce results in qualitative agreement with the experiments, i.e., approximate location of the superconducting phase in a T vs. doping phase diagram, realistic coupling constant values, and dependence with hopping parameters (simulating application of hydrostatic pressure). We find that single-gap SC does not produce acceptable results. This is quite relevant, as there is experimental evidence that BiS₂ presents two gaps²⁷. We find that if we consider s - and p_b -type pairs, and allow for intra and interband scattering we obtain results in semi-quantitative agreement with experiments. The same is true if we choose p_a - and p_b -type pairs, and also allow for intra and interband scattering. The interesting point here is that the t_{sp} hopping is the one that, in both cases, enhances SC when its magnitude in-

creases, whereas the effect on Δ of increasing t_{pp} is marginal. This last point reinforces the need for considering the Sulfur s orbital explicitly. We argue that the anti-symmetric character of the t_{sp} hopping (as stressed in previous work by one of the authors²³) may explain its enhanced effect in the superconducting state.

Acknowledgment. MAC acknowledges *Conselho Nacional de Desenvolvimento Científico e Tecnológico - CNPq* and

Fundaçao de Amparo a Pesquisa do Estado do Rio de Janeiro - FAPERJ for partial financial support; KF acknowledges...; MAG acknowledges financial support from *Conselho Nacional de Desenvolvimento Científico e Tecnológico - CNPq*; and GBM acknowledges the Brazilian Government for financial support through a *Pesquisador Visitante Especial* grant from the *Ciências Sem Fronteiras* Program, from the *Ministério da Ciência, Tecnologia e Inovação*.

- * Corresponding author: griffithmas@hotmail.com
- † Corresponding author: martins@oakland.edu
- ¹ J. G. Bednorz and K. A. Müller, *Zeit. Phys. B-Cond. Matt.* **64**, 189 (1986).
- ² J. Nagamatsu, N. Nakagawa, T. Muranaka, Y. Zenitani, and J. Akimitsu, *Nature* **410**, 63 (2001).
- ³ Y. Kamihara, T. Watanabe, M. Hirano, and H. Hosono, *J. Am. Chem. Soc.* **130**, 3296 (2008).
- ⁴ S.-Z. Lin, *J. Phys. Condens. Matter* **26**, 493202 (2014).
- ⁵ S. R. White and D. Scalapino, arXiv:1503.01533v1 (2015).
- ⁶ C. Beenakker, *Annu. Rev. Condens. Matter Phys.* **4**, 113 (2013).
- ⁷ Y. Maeno, H. Hashimoto, K. Yoshida, S. Nishizaki, T. Fujita, J. G. Bednorz, and F. Lichtenberg, *Nature* **372**, 532 (1994).
- ⁸ A. P. Mackenzie, *Rev. Mod. Phys.* **75**, 657 (2003).
- ⁹ C. Kallin, *Rept. Prog. Phys.* **75**, 042501 (2012).
- ¹⁰ J. Bok and J. Bouvier, *J. Supercond. Nov. Magn.* **25**, 657 (2012).
- ¹¹ S. Raghu, A. Kapitulnik, and S. A. Kivelson, *Phys. Rev. Lett.* **105**, 1 (2010).
- ¹² M. L. Cohen, *Rev. Mod. Phys.* **36**, 240 (1964).
- ¹³ V. Sidorov and E. Ekimov, *Nature* **19**, 351 (2010).
- ¹⁴ Y. Mizuguchi, S. Demura, K. Deguchi, Y. Takano, H. Fujihisa, Y. Gotoh, H. Izawa, and O. Miura, *J. Phys. Soc. Japan* **81**, 114725 (2012).
- ¹⁵ Y. Mizuguchi, *J. Phys. Chem. Solids* pp. 1–15 (2014).
- ¹⁶ J. Liu, D. Fang, Z. Wang, J. Xing, Z. Du, S. Li, X. Zhu, H. Yang, and H.-H. Wen, *Europhys. Lett.* **106**, 67002 (2014).
- ¹⁷ H. Usui, K. Suzuki, and K. Kuroki, *Phys. Rev. B* **86**, 220501 (2012).
- ¹⁸ G. B. Martins, A. Moreo, and E. Dagotto, *Phys. Rev. B* **87**, 081102 (2013).
- ¹⁹ Y. Yang, W. S. Wang, Y. Y. Xiang, Z. Z. Li, and Q. H. Wang, *Phys. Rev. B* **88**, 094519 (2013).
- ²⁰ T. Sugimoto, D. Ootsuki, C. Morice, E. Artacho, S. S. Saxena, E. F. Schwier, M. Zheng, Y. Kojima, H. Iwasawa, K. Shimada, et al., *Phys. Rev. B* **92**, 041113 (2015).
- ²¹ C. T. Wolowiec, B. D. White, I. Jeon, D. Yazici, K. Huang, and M. B. Maple, *J. Phys. Condens. Matter* **25**, 422201 (2013).
- ²² J. E. Hirsch, M. B. Maple, and F. Marsiglio, arXiv:1504.03318 (2015).
- ²³ M. A. Continentino, I. T. Padilha, and H. Caldas, *J. Stat. Mech. Theory Exp.* **2014**, P07015 (2014).
- ²⁴ H. Caldas and M. A. Continentino, *Phys. Rev. B* **86**, 144503 (2012).
- ²⁵ See Supplemental Material at <http://link.aps.org/supplemental/> for the detailed development of the gap equations.
- ²⁶ Most of the studies reporting T_c vs. x results were conducted on polycrystalline samples and the maximum T_c was obtained for $x = 0.5$, corresponding to 0.5 electron per Bismuth, i.e., 1/8-filling, as each Bismuth has two active orbitals (p_x and p_y). Recently, a study on the electronic structure of $\text{NdO}_{1-x}\text{F}_x\text{BiS}_2$ single crystals was reported and it was found that the charge car-

rier doping is smaller than that expected from the nominal x value. This was attributed to Bismuth deficiency⁷. The results we obtain here agree with the nominal concentration (1/8-filling for maximum T_c), which corresponds to 0.25 electron per Bismuth ($\mu = 0.5007$) in the 1d model (with one p orbital per Bismuth).

- ²⁷ D. Yazici, I. Jeon, B. White, and M. Maple, *Physica C Supercond* **514**, 218 (2015).
- ²⁸ T. Tomita, M. Ebata, H. Soeda, H. Takahashi, H. Fujihisa, Y. Gotoh, Y. Mizuguchi, H. Izawa, O. Miura, S. Demura, et al., *J. Phys. Soc. Japan* **83**, 063704 (2014).
- ²⁹ C. T. Wolowiec, D. Yazici, B. D. White, K. Huang, and M. B. Maple, *Phys. Rev. B* **88**, 064503 (2013).
- ³⁰ M. A. Griffith *et. al.*, to be submitted.

I. SUPPLEMENTAL MATERIAL

The gap equations for Δ_1 and Δ_2 are given by

$$\begin{aligned} \Delta_1 &= \Delta_{ss} + \Delta'_{pbpb} \\ &= g_{ss} \sum_k \langle c_{\bar{k}-} c_{k+} \rangle + g_{spb} \sum_k \langle p_{b,\bar{k}-} p_{b,k+} \rangle \end{aligned}$$

and

$$\begin{aligned} \Delta_2 &= \Delta'_{ss} + \Delta_{pbpb} \\ &= g_{spb} \sum_k \langle c_{\bar{k}-} c_{k+} \rangle + g_{pbpb} \sum_k \langle p_{b,\bar{k}-} p_{b,k+} \rangle, \end{aligned}$$

where $\bar{k} = -k$, and the correlation functions are related to the Green's functions (propagators, from now on) $\langle\langle c_{k+}; c_{\bar{k}-} \rangle\rangle$ and $\langle\langle p_{b,k+}; p_{b,\bar{k}-} \rangle\rangle$ through the equation

$$\begin{aligned} \langle\gamma_{\bar{k}-} \gamma_{k+} \rangle &= i \int_{-\infty}^{+\infty} d\omega f(\omega) [\langle\langle c_{k+}; c_{\bar{k}-} \rangle\rangle_{\omega+i\eta} \\ &\quad - \langle\langle c_{k+}; c_{\bar{k}-} \rangle\rangle_{\omega-i\eta}], \end{aligned} \quad (1)$$

where γ stands for the annihilation operators c or p_b , and $\eta \rightarrow 0$. In order to calculate the propagators we will write their equations of motion (taking from now on $\hbar = 1$)

$$\begin{aligned} \omega \langle\langle c_{k+}; c_{\bar{k}-} \rangle\rangle &= \frac{1}{2\pi} \langle\{c_{k+}, c_{\bar{k}-}\} \rangle \\ &\quad + \langle\langle [c_{k+}, H]; c_{\bar{k}-} \rangle\rangle \end{aligned} \quad (2)$$

and

$$\begin{aligned} \omega \langle\langle p_{b,k+}; p_{b,\bar{k}-} \rangle\rangle &= \frac{1}{2\pi} \langle\{p_{b,k+}, p_{b,\bar{k}-}\} \rangle \\ &\quad + \langle\langle [p_{b,k+}, H]; p_{b,\bar{k}-} \rangle\rangle, \end{aligned} \quad (3)$$

where $\mathcal{H}(k)$ is the Hamiltonian for the system (eq. (2) in the main text) and $\{\cdot, \cdot\}$ and $[\cdot, \cdot]$ indicate an anticommutator and a commutator, respectively.

Let us develop further the equation of motion for the first propagator ($\langle\langle c_{k+}; c_{\bar{k}-} \rangle\rangle$). Making use of standard relations for fermion creation and annihilation operators, we obtain

$$\begin{aligned}\omega_s^{(-)} \langle\langle c_{k+}; c_{\bar{k}-} \rangle\rangle &= -2it_{sp} \sin(k) \langle\langle p_{bk+}; c_{\bar{k}-} \rangle\rangle \\ &+ \Delta_1 \langle\langle c_{\bar{k}-}^\dagger; c_{\bar{k}-} \rangle\rangle = 0.\end{aligned}\quad (4)$$

In the process above, two new propagators were created, $\langle\langle p_{bk+}; c_{\bar{k}-} \rangle\rangle$ and $\langle\langle c_{\bar{k}-}^\dagger; c_{\bar{k}-} \rangle\rangle$. In order to close the system of equations for the propagators, we need also the equation of motion for $\langle\langle c_{\bar{k}-}^\dagger; c_{\bar{k}-} \rangle\rangle$, $\langle\langle p_{bk+}; c_{\bar{k}-} \rangle\rangle$, $\langle\langle p_{\bar{b}k-}^\dagger; c_{\bar{k}-} \rangle\rangle$, $\langle\langle p_{ak+}; c_{\bar{k}-} \rangle\rangle$, and $\langle\langle p_{a\bar{k}-}^\dagger; c_{\bar{k}-} \rangle\rangle$. This procedure generates a system of equations given by

$$D \cdot \begin{pmatrix} \langle\langle c_{\bar{k}-}^\dagger; c_{\bar{k}-} \rangle\rangle \\ \langle\langle p_{ak+}; c_{\bar{k}-} \rangle\rangle \\ \langle\langle p_{\bar{a}k-}^\dagger; c_{\bar{k}-} \rangle\rangle \\ \langle\langle c_{k+}; c_{\bar{k}-} \rangle\rangle \\ \langle\langle p_{bk+}; c_{\bar{k}-} \rangle\rangle \\ \langle\langle p_{\bar{b}k-}^\dagger; c_{\bar{k}-} \rangle\rangle \end{pmatrix} = \begin{pmatrix} \frac{1}{2\pi} \\ 0 \\ 0 \\ 0 \\ 0 \\ 0 \end{pmatrix}, \quad (5)$$

where

$$D = \begin{bmatrix} \omega_s^{(-)} & 0 & 0 & \Delta_1 & -\bar{t}_{sp_b} & 0 \\ 0 & \omega_{p_a}^{(+)} & 0 & 0 & 0 & \bar{t}_{p_a p_b} \\ 0 & 0 & \omega_{p_b}^{(-)} & 0 & -\bar{t}_{p_a p_b} & 0 \\ \Delta_1 & 0 & 0 & \omega_s^{(+)} & 0 & \bar{t}_{sp_b} \\ \bar{t}_{sp_b} & 0 & -\bar{t}_{p_a p_b} & 0 & \omega_{p_b}^{(+)} & \Delta_2 \\ 0 & \bar{t}_{p_a p_b} & 0 & -\bar{t}_{sp_b} & \Delta_2 & \omega_{p_b}^{(-)} \end{bmatrix}, \quad (6)$$

and $\omega_q^\pm = \omega \pm \epsilon_q \mp \mu$, $q = s, p_a, p_b$. Here, $\bar{t}_{sp_b} = 2it_{sp_b} \sin(k)$ and $\bar{t}_{p_a p_b} = 2t_{p_a p_b} \cos(k)$.

Using Cramer's method to solve the system of equations in (5), we have that

$$\langle\langle c_{k+}; c_{\bar{k}-} \rangle\rangle = \frac{|D_{ss}|}{|D|} \quad (7)$$

where the matrix D_{ss} is obtained by exchanging the 4th column in matrix D by the column matrix defined in the right side of eq. (5) (note that $|D|$ means the determinant of matrix D). Repeating the same procedure for $\langle\langle p_{bk+}; p_{b\bar{k}-} \rangle\rangle$ we obtain

$$D \cdot \begin{pmatrix} \langle\langle c_{\bar{k}-}^\dagger; p_{b\bar{k}-} \rangle\rangle \\ \langle\langle p_{ak+}; p_{b\bar{k}-} \rangle\rangle \\ \langle\langle p_{\bar{a}k-}^\dagger; p_{b\bar{k}-} \rangle\rangle \\ \langle\langle c_{k+}; p_{b\bar{k}-} \rangle\rangle \\ \langle\langle p_{bk+}; p_{b\bar{k}-} \rangle\rangle \\ \langle\langle p_{\bar{b}k-}^\dagger; p_{b\bar{k}-} \rangle\rangle \end{pmatrix} = \begin{pmatrix} 0 \\ 0 \\ 0 \\ 0 \\ 0 \\ \frac{1}{2\pi} \end{pmatrix} \quad (8)$$

where

$$\langle\langle p_{-k}; p_k \rangle\rangle = \frac{|D_{pbpb}|}{|D|}. \quad (9)$$

and D_{pbpb} is obtained by exchanging the 5th column in matrix D by the column matrix defined in the right side of eq. (8). In eqs. (7) and (9), $|D|$ is a biquadratic polynomial of degree six and can be rewritten as

$$\begin{aligned}|D| &= \sum_{n=0}^3 B_{2n} \omega^{2n} = \prod_{n=1}^6 (\omega - \omega_n) \\ &= \prod_{n=1}^3 (\omega^2 - \omega_n^2)\end{aligned}\quad (10)$$

where the last equation is obtained by noting that $\omega_1 = -\omega_4$, $\omega_2 = -\omega_5$, and $\omega_3 = -\omega_6$. Here, A_n and B_n are coefficients which are functions of the parameters of the Hamiltonian. ω_n are the zeros of $|D|$ and represent the energy excitations of the system. The solutions for $\omega_k \equiv \omega$ cannot be found analytically. Actually, these quantities will be obtained numerically.

To finally determine the gap equations, it is appropriate to make use of the following identity

$$\begin{aligned}\frac{1}{|D|} &= \frac{1}{r_1} \left[\frac{1}{2\omega_1} \left(\frac{1}{\omega - \omega_1} - \frac{1}{\omega + \omega_1} \right) \right] \\ &+ \frac{1}{r_2} \left[\frac{1}{2\omega_2} \left(\frac{1}{\omega - \omega_2} - \frac{1}{\omega + \omega_2} \right) \right] \\ &+ \frac{1}{r_3} \left[\frac{1}{2\omega_3} \left(\frac{1}{\omega - \omega_3} - \frac{1}{\omega + \omega_3} \right) \right],\end{aligned}\quad (11)$$

where

$$\begin{aligned}r_1 &= (\omega_1^2 - \omega_2^2)(\omega_1^2 - \omega_3^2) \\ r_2 &= (\omega_2^2 - \omega_1^2)(\omega_2^2 - \omega_3^2) \\ r_3 &= (\omega_3^2 - \omega_1^2)(\omega_3^2 - \omega_2^2).\end{aligned}$$

Substituting eq. (11) into eqs. (7) and (9), and after using eq. (1), we have

$$\begin{aligned}\langle\gamma_{-k}\gamma_k\rangle &= i \sum_{j=1}^3 \int_{-\infty}^{+\infty} d\omega f(\omega) \frac{D_{\gamma\gamma}(\omega)}{2\omega_j r_j} \\ &\times (C_+(\omega) - C_-(\omega)),\end{aligned}\quad (12)$$

where we have defined the following quantities

$$C_\pm(\omega) = \lim_{\eta \rightarrow 0^+} \left(\frac{1}{\omega \pm \omega_j - i\eta} - \frac{1}{\omega \pm \omega_j + i\eta} \right). \quad (13)$$

Now, using the fact that

$$\delta(x) = \frac{1}{2\pi i} \lim_{\eta \rightarrow 0^+} \left(\frac{1}{x - i\eta} - \frac{1}{x + i\eta} \right), \quad (14)$$

we finally get

$$\begin{aligned}\langle\gamma_{-k}\gamma_k\rangle &= \pi \sum_{j=1}^3 \frac{|D_{\gamma\gamma}(\omega_j)| f_{FD}(\omega_j)}{\omega_j r_j} \\ &- \pi \sum_{j=1}^3 \frac{|D_{\gamma\gamma}(-\omega_j)| f_{FD}(-\omega_j)}{\omega_j r_j},\end{aligned}\quad (15)$$

where $f_{FD}(\omega_j) = \frac{1}{\exp(\omega_j/k_B T) + 1}$.

Substituting eq. (15) into the equations for Δ_1 and Δ_2 in the previous page, and taking the limit $T \rightarrow 0$, we can write the following self-consistent equations

$$\begin{aligned}\Delta_1 &= \Delta_{ss} + \Delta'_{p_b p_b} \\ &= -g_{ss} \sum_k \pi \sum_{j=1}^3 \frac{|D_{ss}(-\omega_j)|}{\omega_j r_j} \\ &\quad - g_{sp_b} \sum_k \pi \sum_{j=1}^3 \frac{|D_{p_b p_b}(-\omega_j)|}{\omega_j r_j}\end{aligned}\quad (16)$$

and

$$\begin{aligned}\Delta_2 &= \Delta'_{ss} + \Delta_{p_b p_b} \\ &= -g_{sp_b} \sum_k \pi \sum_{j=1}^3 \frac{|D_{ss}(-\omega_j)|}{\omega_j r_j} \\ &\quad - g_{p_b p_b} \sum_k \pi \sum_{j=1}^3 \frac{|D_{p_b p_b}(-\omega_j)|}{\omega_j r_j}.\end{aligned}\quad (17)$$

In the thermodynamic limit ($L \rightarrow \infty$), we can replace the sum by an integral [in the interval $-k_f \leq k \leq k_f$] by using the standard relation

$$\frac{2\pi}{L} \sum_k \Delta_k = \frac{1}{2\pi} \int_{-k_f}^{k_f} dk,\quad (18)$$

where, k_f is the Fermi-wavevector and L is the length of the one-dimensional system. For practical purposes, we change the integration variable ($\tilde{k} = k/k_f$), and finally write

$$\begin{aligned}\Delta_1 &= -g_{ss} k_f \pi \int_{-1}^1 d\tilde{k} \sum_{j=1}^3 \frac{|D_{ss}(-\omega_{\tilde{k},j})|}{\omega_{\tilde{k},j} r_j} \\ &\quad - g_{sp_b} k_f \pi \int_{-1}^1 d\tilde{k} \sum_{j=1}^3 \frac{|D_{p_b p_b}(-\omega_{\tilde{k},j})|}{\omega_{\tilde{k},j} r_j},\end{aligned}\quad (19)$$

and

$$\begin{aligned}\Delta_2 &= -g_{sp_b} k_f \pi \int_{-1}^1 d\tilde{k} \sum_{j=1}^3 \frac{|D_{ss}(-\omega_{\tilde{k},j})|}{\omega_{\tilde{k},j} r_j} \\ &\quad - g_{p_b p_b} k_f \pi \int_{-1}^1 d\tilde{k} \sum_{j=1}^3 \frac{|D_{p_b p_b}(-\omega_{\tilde{k},j})|}{\omega_{\tilde{k},j} r_j}.\end{aligned}\quad (20)$$

In a one-dimensional system, $k_f = \frac{\rho\pi}{2}$, where $\rho = \frac{N}{L}$ is the density of electrons in the material and N is the total number of electrons. Note that, when $g_{ss} = g_{p_b p_b} = g_{sp_b}$, we have $\Delta_1 = \Delta_2$.